Al-Kitab Journal for Pure Sciences (2023); 7(2):99-114.
https://doi.org/10.32441/kjps.07.02.p9

Al-Kitab Journal for Pure Sciences
ISSN: 2617-1260 (print), 2617-8141(online)
https://isnra.net/index.php/kjps

Using Universal Kriging for Spatiotemporal Data of Soil Pollution with Metals in Al Karama Industrial Area in Mosul City

Mai Hussein Ali *, **Ghanim Mahmood Dhahir**

Department of Mathematics, College of Education for Pure Sciences, University of Mosul, Mosul, Iraq.

*Corresponding Author: mustafamohamed40020@gmail.com

Citation: Ali MH, Dhahir GM. Using Universal Kriging for Spatiotemporal Data of Soil Pollution with Metals in Al Karama Industrial Area in Mosul City. 2023 Oct 30;7(2):99-114. Available from: https://doi.org/10.32441/kjps.07.02.p9.

Keywords: The Universal Kriging, the Covariance models, Spatiotemporal data, standards of error.

Article History

Received	03 Sep. 2023
Accepted	22 Oct. 2023
Available online	30 Oct. 2023

Abstract:

The current research tackles the performance of Spatiotemporal Interpolation Techniques using the Kriging Technique after relating it to time, which is introduced to the Prediction Process as the reliable mathematical formula to obtain the best performance of a proposed mathematical model. This study's main objective is to evaluate the best Unbiased Linear Prediction Technique with the slightest variance of error through mathematical equations that are derived and related to time.

In this study, the researcher used Spatiotemporal Data of Soil Pollution with minerals in the industrial zone in Mosul city with the actual locations. The data consists of (192) real observations of Arsenic (As) and Chrome (Cr) in the AL Karama Industrial Zone, and this data represents the depth with the actual locations. The Kriging Technique and Kriging Covariance through the mathematical formula are related to time in this research. A function for the place was applied, namely, the variogram function that represents the difference between the observations, as this function was determined for all the directions of the compass, and its parameters were estimated. Through the covariance and the standards of error, it was concluded that the ideas of the Mathematical Spatiotemporal model express the positivity of the proposed model amongst the models of the Covariance functions, such as the Spherical model and the

Exponential model, which are approximate models from the principal point of view to the characteristics of the Kriging mode. We also recommend entering three-dimensional data to obtain a proposed mathematical model or data for infectious diseases and atmospheric gas Pollution, using other Spatiotemporal Prediction methods and linking them with artificial intelligence and Fuzzy methods. All the calculations were conducted using the MATLAB Language.

Keywords: The Universal Kriging, the Covariance models, Spatiotemporal data, standards of error.

استخدام الكريكنك الشامل للبيانات الزمانية المكانية لتلوث التربة بالمعادن في منطقة الكرامة الصناعية في مدينة الموصل

مي حسين علي *، غانم محمود ظاهر
ghanim-hassod@uomosul.edu.iq ، mustafamohamed40020@gmail.com

قسم الرياضيات، كلية التربية للعلوم الصرفة، جامعة الموصل، العراق.

الخلاصة:

يتناول هذا البحث أداء تقنيات الاستكمال الزماني المكاني باستخدام تقنية كريكنك بعد ربطها بالزمن والتي تدخل في عملية التنبؤ على شكل صيغ رياضية معتمدة من أجل الحصول على أفضل أداء لنموذج رياضي مقترح. إن الهدف الرئيسي من هذه الدراسة هو تقييم أفضل لتقنية التنبؤ من أجل الحصول على أفضل تنبؤ خطي غير متحيز مع أقل تباين للخطأ من خلال معادلات رياضية مشتقة ومرتبطة بالزمن.

لقد تم الاعتماد في هذا البحث على بيانات زمانية ومكانية لتلوث التربة بالمعادن في منطقة صناعية في مدينة الموصل مع مواقعها الحقيقية حيث تتكون البيانات من (١٩٢) مشاهدة حقيقية لكل من معدني الزرنيخ (*As*) والكروم (*Cr*) في صناعة الكرامة وهذه البيانات تمثل العمق مع مواقعها الحقيقية. من خلال هذا البحث تم تطبيق تقنية كريكنك وتباين كريكنك من خلال الصيغ الرياضية المرتبطة بالزمن. وقد تم تطبيق دالة للموقع ودالة للزمن هي دالة الفاريوكرام والتي تمثل الفرق بين المشاهدات حيث تم احتساب هذه الدالة لجميع اتجاهات البوصلة وتقدير معلمات الدالة. وتم من خلال النتائج التوصل إلى أن تقنية كريكنك تظهر أداءً وتقديراً مميزاً وواقعياً وذلك من خلال صيغ التباين ومعايير صحة الخطأ. إن أفكار النموذج الرياضي الزماني المكاني المشترك يعبر عن إيجابية النموذج المقترح من بين نماذج دوال التغاير مثل النموذج الكروي والنموذج الأُسي وهما نموذجان متقاربان من حيث المبدأ لخصائص تقنية كريكنك. كما نوصي بإدخال بيانات ثلاثية الأبعاد للحصول على نموذج رياضي مقترح، أو بيانات لأمراض العدوى والتلوث بالغازات الجوية، واستخدام طرق تنبؤ زمكانية أخرى وربطها مع أساليب الذكاء الاصطناعي أو الأسلوب المضبب. تم إجراء الحسابات باستخدام لغة ماتلاب (*Matlab Language*).

الكلمات المفتاحية: الكريكنك الشامل، نماذج التغاير، بيانات زمانية مكانية، معايير الخطأ.

1. Introduction:

Kriging Technique gained this name after the name of the South African mining engineer D. G. Krige, who submitted specific ideas in his master's thesis in (1951), and these ideas were adopted by the famous French mathematician George Matheran and called the Kriging Technique for spatial prediction. Spatial prediction received significant attention in statistics as the forecast can potentially affect the values in unknown locations. Despite the long history of this subject, the uncertainty feature is related to the type of the most convenient prediction method. Sometimes, many researchers rely on the nature of the data (samples) and the decisions made when identifying the prediction criteria. When any vector is specified, a particular indicator can be measured by increasing the number of Kriging applications, and it is the Best Linear Unbiased Prediction (BLUP)m where the statistical characteristic is preferred repeatedly so that the chance is available to determine the mean as a model in Kriging Technique. Usually, the spatial technique is evaluated into two values: mean and residual. Here, the random data is related to the residual, and the Universal kriging (UK) becomes related to the mean. Several studies suggest a model estimate the level of air pollution explicitly by merging both the temporal and spatial dependent variables; spatial interpolation methods and their applications have been developed in various disciplines, such as mining engineering **[11]** and environmental sciences **[6]**, **[1]**, many studies have dealt with spatial prediction **[5]**, **[15]**, in health, pollution and precipitation **[16]**, in the field of soil data, its properties and groundwater **[3]**, **[2]**.

2. Method

2.1 Regionalized Random Variables:

If the random variable Z(s) is a spatial variable in the location s, and if $s = s_o$, then $Z^*(s_o)$ is the variable to be predicted in the location s_o. The random spatial variable (regional) is defined as a numerical function with a spatial distribution that is different from one location to another with the continuity of the phenomenon, but the spatial (regional) data is the information that describes objects and events in a location of the earth surface or near it or inside the earth or close to it. Usually, the spatial geographical data involves the information of the location (it includes coordinates on the ground, the feature or the event information, or certain phenomena) with the temporal information (time or age) that exists in the location, and the location is stable on the wide range. If Z(s) is a random spatial variable in the location (s), then the distribution data Z(s) has a prediction that is written with the following formula:

$$\mathbf{m(s) = E[Z(s)] = \int_{-\infty}^{\infty} x\, f_{Z(s)}(x)dx = \mu} \qquad \mathbf{, \forall\, s \in D} \qquad \mathbf{(1)}$$

his case is called First-Order Stationarity, but in Second-Order Stationarity, the random variable Z(s) is a second-order stationary variable if the prediction of the random variable is present and doesn't depend on the location (s). $\boldsymbol{E[Z(s)] = \mu \quad , \ \forall s \in D}$

If the variance exists, it is defined as $\mathbf{var\ [Z(s)] = \ \sigma^2_{Z(S)} = E[\{Z(s) - m(s)\}^2]}$

$$\mathbf{var\ [Z(s)] = \int_{-\infty}^{\infty} (x - m(s))^2\, f_{Z(s)}(x)\, dx}$$

For each pair of spatial random variables $[\boldsymbol{Z(s), Z(s+h)}]$ The covariance function is known and depends on lag only.

$$\mathbf{COV\ \big(Z(s), Z(s+h)\big) = \ E\big[\big(Z(s) - \ m(s)\big)\big(Z(s+h) - \ m(s+h)\big)\big] \ = \ \sigma\ (h)}$$

The second-order stationarity entails the presence of the covariance function and a specific finite variance function. The Intrinsic Stationary is more generalized than the previous stationarity in that the mathematical prediction exists and doesn't depend on the location (s).

$$\mathbf{E\ [Z(s)] = \ \mu}$$

The increase $[\mathbf{Z(s), Z(s+h)}\ ]$ has a finite variance and doesn't depend on the location (s).

$$\boldsymbol{var[Z(s), Z(s+h)] = \ E[(Z(s+h) - \ Z(s))^2] = \ 2\gamma(h)}$$

The function $2\gamma(h)$ is called a variogram function, while the stochastic process is called the random process, which is a group of random variables that depend on time. If we assume that there is the element (s) (sample space) for a random experiment (E), then the function:

$$\boldsymbol{Z = \{Z(t,s), t\ \epsilon T\ , s\ \in\ S\}, T\ \subset\ R} \qquad \textbf{(2)}$$

It is called the random process or the stochastic process.$\big((t), (t,s)\big)$, where T is the parameter time, S is the space, and the sample (the case) (states space), as T might be countable (discontinuous values) or uncountable (continuous) ,and the same is with s [8], [13], [17].

2.2 Variogram Function:

Usually, the variogram function is defined as the function of the following probabilities:

$$\mathbf{2\gamma(h) = E[(Z(s) - Z(s+h))^2]} \qquad \textbf{(3)}$$

When dealing with the real data, the variogram function is estimated by the experimental variogram function in relation to the lag vector (h) as a set of observations that exist in the form of pairs with spaces between them lag(h) [4], [7], [9].

$$\boldsymbol{2\gamma^*(h) = \frac{1}{N(h)} \sum_{i=1}^{N(h)} (Z_i - Z_j)^2, j=1,2\ldots,N(h)} \qquad \textbf{(4)}$$

There are three parameters for the variogram function, they are:

- The range is symbolized with (a), and it represents the distance on the x coordinate or lag until the curve is stable.
- Sill, where the value of $\mathbf{c + c_o}$ Represents the variance.

- The Nugget Effect stands for the random errors in the measurement units, which is the nugget effect of the function at h = 0, and it is also called the nugget effect or discontinuity, as shown in **Figure (1)**:

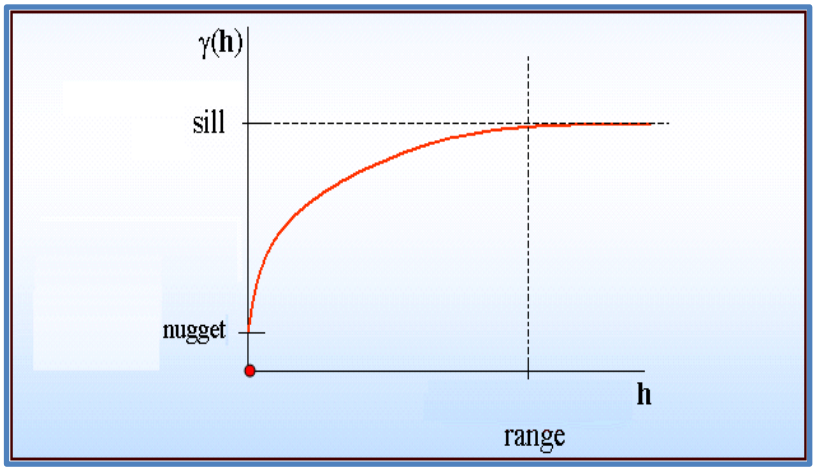

Figure (1): An illustration of the variogram function characteristics

Figure (1) shows the variogram drawing in general, where the x-axis is the lag(h) and the y-axis represents the semi-variogram function γ(h) with the parameters: (nugget effect) is the lack of continuity, (still) is the variance, and (range) is the lag. The variogram function has the following properties:

$$\boldsymbol{\gamma(h) = \gamma(-h)}$$
$$\boldsymbol{\gamma(0) = 0} \qquad \boldsymbol{, h = 0}$$
$$\boldsymbol{\frac{\gamma(h)}{\| h \|^2} \to 0} \qquad \textbf{when} \qquad \boldsymbol{\|h\| \to \infty}$$

For any real group $\{a_1, a_2, \dots\dots\dots, a_n\}$ that verifies $\sum_{i=1}^{m} \mathbf{a_i} = \mathbf{0}$ we get the following characteristics: $\boldsymbol{\Sigma_{i=1}^{m} \Sigma_{j=1}^{m} a_i \; a_j \; \gamma\left(s_i - s_j\right) \leq 0}$

Here, the process is isotropic, i.e., $\boldsymbol{\gamma(\mathbf{h}) = \gamma(\|h\|)}$. There is a relationship that connects the variogram and the covariance function, which $\boldsymbol{\gamma(\mathbf{h}) = \mathbf{C}(\mathbf{0}) - \mathbf{C}(\mathbf{h})}$, where γ(h) is Semi variogram function and C(0) is a Variance function and C(h) represents the Covariance function **[4] ,[7]** .

2.3 Spatiotemporal Random Function Model

Let $Z = \{Z(s,t), s \in S, t \in T\}$ be a group of spatiotemporal data or temporal data from a variable with spatial coordinates $(s_i, t_i), i = 1, \dots\dots, n$ within the spatial domain S for the time interval T. Assuming that this definition satisfies the stochastic spatiotemporal function $Z(s,t)$, predictions can be made $Z(s_o, t_o)$ For the unmeasurable spatiotemporal points **[6],** the model of the random function is given as follows:

$$\boldsymbol{Z^*(s,t) = m(s,t) + e(s,t)} \qquad \textbf{(5)}$$

Where m (s, t) is the deterministic part and e (s, t) is the stochastic residual part. The stability of the direction can be presumed in the time and place, and it can be allowed to change as a known function of covariates, and m represents the basic variance in the spatiotemporal process. The direction is developed by the regression-type model that connects the important variable z with the relevant covariates. The residual **e** represents the difference between the observations and predictions of the trend of the stationarity model of residuals for replication in Kriging processes results from removing the direction component, and they are distributed normally [7], [18], [17].

2.4 Spatiotemporal Variogram Function

The estimation of spatiotemporal direction is done by subtracting m(s) from the observations of the spatiotemporal level e(s, t), and the residual might be differences or correlations in space and time. The resulting residuals could be used in constructing the sample of the variogram function in time and space. The sample of the variogram function model diagram $2\gamma(h,u)$ is calculated as follows:

$$\boldsymbol{2\gamma(h,u) = \frac{1}{N(h,u)}\sum_{i=1}^{N(h,u)} [e(s,t) - e(s+h,t+u)]^2} \quad \textbf{(6)}$$

Where h is the distance separating the points in space and, u is the separation in the time, N(h, u) is the number of observations in Z that are separated by lag (h, u). The spatiotemporal structure of the variogram function is symbolized by $2\gamma(h,u)$, which is according to the distance or lag. Once the plot samples of the spatiotemporal variogram function model are calculated, a model with a few model variances can be modeled to estimate the spatiotemporal covariance and variance. The variogram function can represent the spatiotemporal variables. $\gamma_{S,T}(s,t)$ in the following formula:

$$\boldsymbol{\gamma_{S,T}(s,t) = \gamma_s(h) + \gamma_T(u) + \gamma_J\left(\sqrt{h^2 + (x,u)^2}\right)} \quad \textbf{(7)}$$

Where x represents the spatiotemporal variance when the spatiotemporal distances and the spatial distance are merged, and γ_J Are the spatiotemporal variogram functions [19], [21].

2.5 Universal Kriging

In this type of kriging, the data Z_i, i= 1, …, n, are unknown at the points *vi* where i= 1, …, n is interpreted as outcomes of a random field that can be decomposed as the sum of the deterministic components of a random field Z(s) is stationarity and has a mean of zero. This is supposed to be*:* $\mathbf{Z(s) = \sum_{j=1}^{P} \beta_j f_j(s) + R(s)}$

Where R is a zero mean of a random field, which is represented as a function *f*, which is assumed to be known, together with the variogram function of the random field R, the

coefficients β_j are secondary coefficients of the prediction. Under these assumptions, Universal Kriging (UK) can be defined as If we have s_o, then Universal Kriging overall estimate at a point s_o based on the spatial data $Z(s_i)$ where $i = 1, \ldots, n$ is defined as an unbiased linear estimate.

$$Z^*(s_0) = \sum_{i=1}^{n} \lambda_i Z(s_i)$$

With the most accurate squared predictive error. The Universal Kriging can be written in the following form: $\mathbf{Z = X\beta + R}$

Justifying the morphological similarity with the general linear estimation. The function to be minimized can be written in the case of a Universal Kriging as follows:

$\varphi(\lambda_1, \lambda_2, \ldots, \lambda_n, m_1, \ldots, m_p) = E[(Z(s_0) - \sum_{i=1}^{n} \lambda_i Z(s_i))^2] - 2\sum_{j=1}^{p} m_j(\sum_{i=1}^{n} \lambda_i f_j(s_0))$,Where $j = 1, \ldots, p$ and m_j Are Lagrangian multiples, repeating the derivation along the lines of the above leads to a linear system. $\lceil U\, \lambda U = \gamma U$, where $\lceil U$ is a matrix, λU is a value, and γU is a value. The Universal Kriging Coefficients can be determined by solving the linear system. $\lceil U\, \lambda U = \gamma U$, therefore: $\lambda U = \lceil_U^{-1}\, \gamma U$.

Similarly, the squared prediction error can be calculated as in the case of Ordinary Kriging (OK) through the following equation [9], [10], [14].

$$\sigma_{UK}^2(v_0) = \lambda_U^T\, \gamma U = \gamma_U^T\, \lceil_U^{-1}\, \gamma U \qquad (10)$$

2.6 Spatiotemporal Kriging Technique

In a similar way to the pure spatial case in the regression Kriging (RK), separate predictions are of the direction, and the remaining components are performed, and then they are added together once again. The techniques of applying the steps differ in terms of satisfying the Spatiotemporal Kriging Technique (STK) on the random residuals through the best unbiased linear prediction $e(s_o, t_o)$.

$$e^*(s_o, t_o) = \sum_{i=1}^{n} \lambda_i e(s_i, t_i) \qquad (9)$$

where; λ_i Represents the weights of the spatiotemporal Kriging technique that is determined by the spatiotemporal waste structure. Also, $e(s_i, t_i)$ Are the residual of the samples in the area that is neighboring the prediction location? The optimum weights of the spatiotemporal Kriging technique are obtained via the following relation:

$$\sum_{i=1}^{n} \lambda_j \gamma_{st}(s_i - s_j, t_i - t_j) + \mu = \gamma_{st}(s_i - s_o, t_i - t_o), \qquad \forall_j = 1, \ldots, n$$

$$\sum_{i=1}^{n} \lambda_i = 1$$

Where the Lagrange multiplier μ is the number of observations that are confined to the research area. The final spatiotemporal estimation in the location (s_o, t_o) It is given by the components that remain together.

$$\boldsymbol{Z^*(s_o, t_o) = m^*(s_o, t_o) + e^*(s_o, t_o)} \quad \textbf{(11)}$$

The prediction covariance is estimated by:

$$\boldsymbol{var(Z^* s_o, t_o) - Z(s_o, t_o)) = \sigma^2\left(m^*(s_o)\right) + \left(\sum_{i=1}^{n} \lambda_i\ \gamma_{s,t}(s_i - s_o, t_i - t_o) + m\right)}$$

The vector of the error component is given by:

$$\boldsymbol{\sigma^2\left(m^*(s_o)\right) = (x_o - x^T\ c^{-1}\ c_o)^T (x^T\ c^{-1}\ x)^{-1}\ (x_O - x^T\ c^{-1}\ c_O)} \quad \textbf{(12)}$$

Where *x* is the sample of the covariance matrix remaining in the research locations, c is the covariates in the research location, and x_o It is the vector of the variables [12], [20], [17].

2.7 Measures of The Predictive Performance with Time

The predictive performance for each model is accomplished by verifying the (Cross Validation) as the accuracy of prediction validity with the time factor by the mean absolute predictive error (MAPE), which equals:

$$\boldsymbol{MAPE = \frac{1}{N} \sum_i \sum_t \left| \frac{\gamma(s_i, t) - \gamma^*(s_i, t)}{\gamma^*(s_i, t)} \right| * 100} \quad \textbf{(13)}$$

Where N is the total number of available observations in the group, $\gamma(s_i, t)$ is the measurements of the pollution in the counter i and the unit of time in the group t, $\gamma^*(s_i, t)$ Represents the root mean square error (RMSE) can be found [20]:

$$\boldsymbol{RMSE = \sqrt{\frac{1}{N} \sum_i \sum_t \left(\gamma(s_i, t) - \gamma^*(s_i, t)\right)^2}} \quad \textbf{(14)}$$

3. Data Analysis

We relied on spatiotemporal data with their actual locations from research published in the College of Environmental Sciences by researcher Salem Rabie Zannad (2020), and the title of the research was "Industrial Pollution and Environmental Impact Assessment of Industrial Areas in the City of Mosul." University of Mosul.

3.1 The area of study

The area of the study is in Mosul city in the northern west part of Iraq, which is between the longitude 41 º - 44º to the east and latitude of (41º - 44º) to the east and latitude of (35º - 37º). The Al Karama industrial zone is in the eastern part of Mosul (the left bank of the city). The area of the study is famous for the factories and mills in addition to the repair and maintenance shops and garages that represent an important factor to the city. The real spatiotemporal data of the industrial zone in Mosul city is the data adopted in this research, and it consists of (192)

real values for Arsenic (As) and Chrome (Cr), which cause pollution to the soils of the industrial zone with the course of time and for three seasons: (Autumn, Winter, and Spring).

Table (1): Results of the variogram functions for Arsenic and Chrome metals for all the trends

Arsenic As							
G1	0.932	1.260	1.491	2.093	3.151	3.796	5.108
G2	7.096	14.640	18.552	21.829	22.486	16.377	30.059
G3	8.373	17.082	20.769	26.197	31.531	28.323	52.590
G4	6.243	13.054	16.192	18.917	17.085	9.182	12.410
G5	4.014	7.950	10.022	11.961	12.819	10.086	17.583
G6	7.308	15.068	18.480	22.557	24.308	18.753	23.500
Chrome Cr							
G1	0.364	0.322	0.270	0.380	0.602	0.481	0.656
G2	0.425	1.040	1.880	3.130	4.222	5.547	7.119
G3	0.618	1.336	2.521	4.126	5.326	6.718	7.507
G4	0.410	0.819	1.136	2.180	3.496	2.914	2.722
G5	0.848	1.340	1.968	2.957	3.888	5.075	6.580
G6	1.153	2.098	3.118	5.204	7.160	7.502	6.250

Table (1) below contains the results of the variogram function according to equation (1) for all the directions of the compass with the basic angles of the compass (θ=135°, 45°, 90°, 0°), where G1 represents the angle θ=0°, G2 represents the results at the angle θ=90° with lag (h), whereas G3 stands for the results at the angle θ=45° and G4 represents the results at the angle θ=135° with lag (h) of h = 1.414, 2.82, …, 9.898 for the case of Arsenic and Chrome metals. The results of the mean variogram function where the first row is G5 represents the mean of the two angles θ = 90°, 0° because the lag is equal when h =1, 2, …,7, the second row shows the mean of the two angles θ = 135°, 45° because the lag is equal in the case of the Arsenie and the Chrome metals.

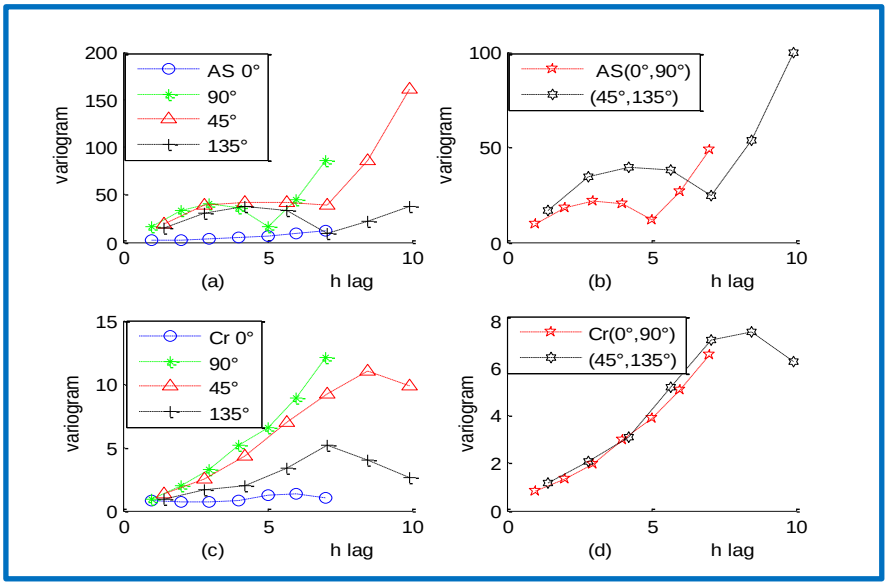

Figure (2): Curves of the variogram function for the Arsenic and Chrome metals

Figure (2) shows the curves of the variogram functions as the curves in (a) for all the angles: the blue curve is when θ=0°, the green curve is when θ = 90°, the red curve is when the angle is (θ=45°) and the discontinuous dots curve is when θ =135°. As for (b), it represents the mean of the two variogram functions at the angles (0°and 90°) represented by the red curve, and the black curve represents the angles (45° and 135°) for Arsenic (As). The same can be said for the curves in figure (c) for all the angles related to Chrome, and figure (d) represents the mean variogram function of Chrome.

Table (2): Results of the characteristics of the variogram function means for Arsenic and Chrome metals for all the angles.

Metal / Statistics	As		Cr	
	(0°,90°)	(45°,135°)	(0°,90°)	(45°,135°)
Min	4.014	7.308	0.848	1.154
Max	17.58	32.5	6.58	7.503
Mean	10.63	19.85	3.237	4.641
Median	10.09	18.75	2.958	5.204
Range	6	8.485	6	8.485

Table (2) shows the results of the variogram function for all the angles, where (Min) stands for the point of nugget effect, (Max) represents the variance, (Mean) represents the mean, (median) represents the median, and (Range) stands for the range in the case of Arsenic and Chrome metals.

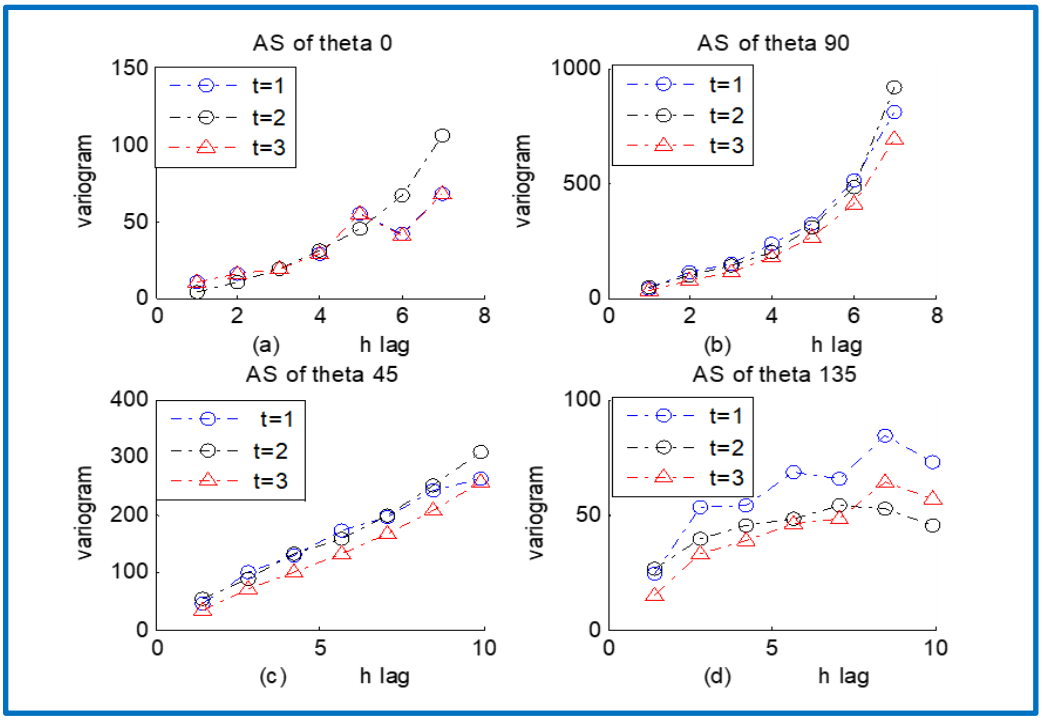

Figure (3): Results of variogram function of the spatiotemporal data of Arsenic and Chrome metals in all the directions of the compass

Figure (3) shows the variogram functions, where (a) represents the result of the variogram function at the angle (0^o) with time. Where (t =1, t=2, t=3) between the lag on the x-axis and the variogram function on the y-axis and the same is for the rest of the angles in the figure; (b), (c) and (d) for the angles 45, 90 and 125 ^{o} respectively. In **Figure (3)**, the curves of the functions (a) as (t=1, t=2, t=3) between the lag on the x-axis and the variogram function on the y-axis and the same for the rest of the angles in figures b, c and d for the angles (45°, 90°, and 135°) respectively.

Table (3): Results of the variogram function mean of Arsenic metal at (t=1, t=2, t=3)

G5 (T=1)	G6(T=2)	G7(T=3)
9.667	9.224	9.828
19.753	18.248	20.070
24.566	21.415	24.895
23.881	20.355	25.404
13.380	11.818	14.965
31.483	26.882	34.139
60.007	48.866	66.623

Table (3) shows the results of the variogram function mean, where G5 represents the results of the variogram function mean at (T=2), and G7 represents the variogram function mean at (T=3).

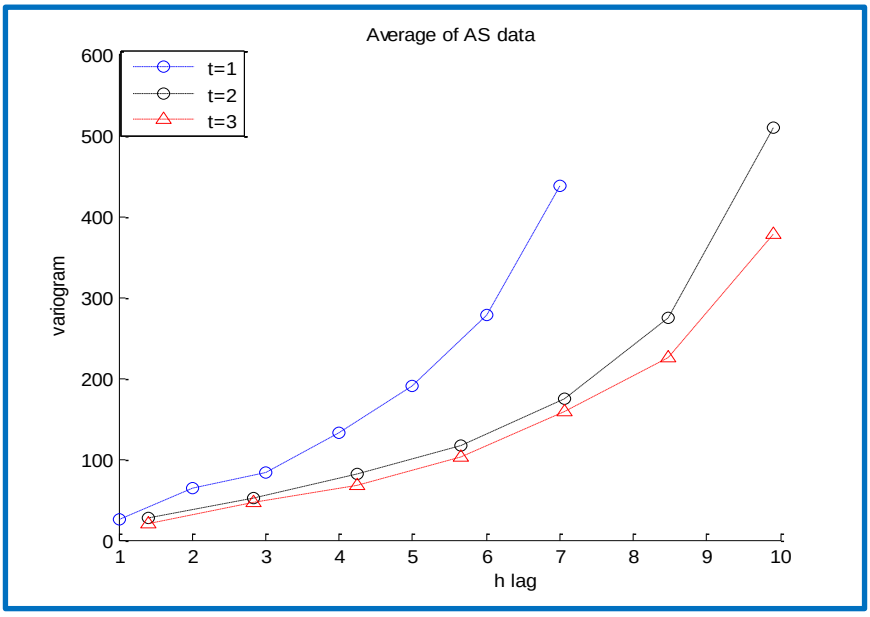

Figure (4): Results of variogram mean of the spatiotemporal data of Arsenic.

Figure (4) shows three curves of the variogram. The blue curve shows the average at (t=1), the red curve shows the average at (t = 2), and the black curve shows the average at (t=3).

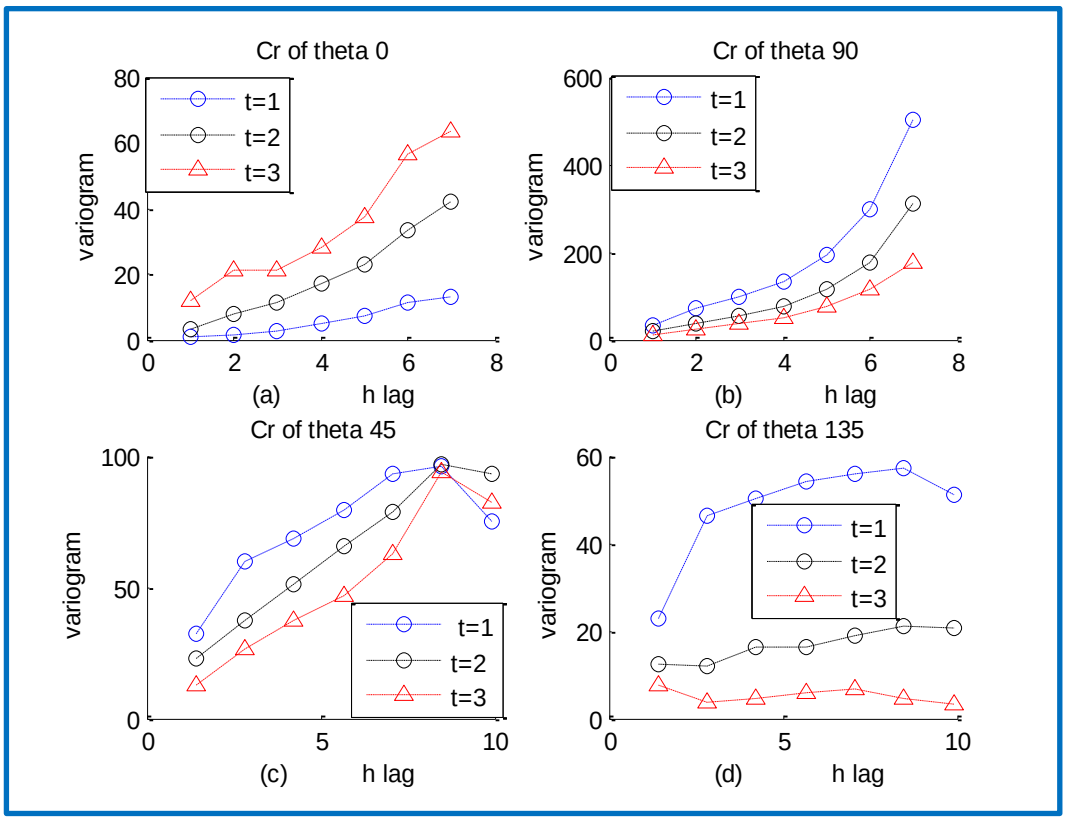

Figure (5): of the spatiotemporal data of Chrome in all the directions of the compass

Figure (5) shows the curves of the variogram functions. Part (a) represents the Results of the variogram function at the angle (0^o) with the times (t = 1, t = 2, t = 3) between the lag on the x-axis and the variogram function on the y-axis. The same is true for the rest of the angles in the parts (b), (c), and (d) in the figure for the angle.

Table (4): variogram function of the mean of Chrome.

G5 (t=1)	G6(t=2)	G7(t=3)
0.789	0.848	0.803
1.363	1.340	1.284
2.150	1.968	1.917
3.511	2.957	2.841
4.825	3.888	3.865
6.029	5.075	5.383
7.775	6.580	6.940

Table (4) represents the results of the mean variogram function at time (t = 1,2,3). G5 represents the mean of the angle (0^o), G6 represents the mean of the angle (90^o), and G6 represents the mean of the angle (45^o).

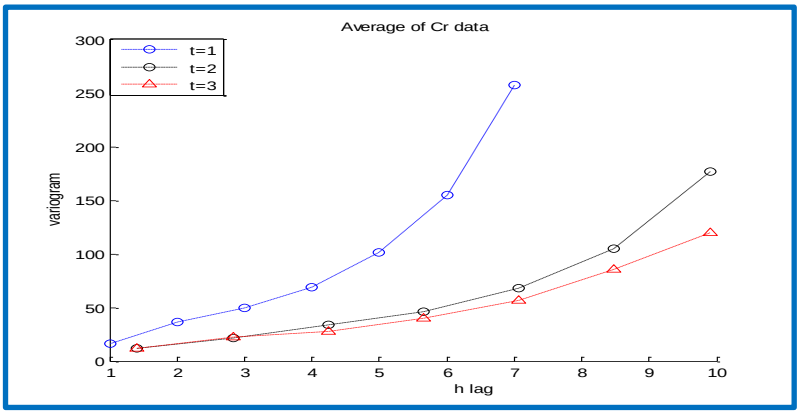

Figure (6): Results of an average of variogram function at (t=1, t=2, t=3) for Chrome

Figure (6) includes three curves of the mean variogram function for Chrome. The blue curve shows the mean at (t = 1), the black curve shows the mean at (t = 2), and the black curve shows the mean at (t = 3).

Table (5): Results of the variogram function characteristics for Arsenic and Chrome at (t=1, t=2, t=3)

Statistics \ Time	As			Cr		
	t=1	t=2	t=3	t=1	t=2	t=3
Min	25.73	26.64	20.06	16.01	12.21	11.96
Max	437.8	509.6	378.9	257.8	176.7	120
Mean	173	176.7	142.7	97.73	66.23	52.14
Median	132.3	116	102.3	68.67	46.39	39.49
Range	6	8.485	8.485	6	8.485	8.485

Table (5) shows the results of the variogram function characteristics for all the times (t=1, t = 2, and t=3) for the average of the variogram function for Arsenic and Chrome. Min represents the nugget effect point; Max represents the variance. Mean represents the average, Median, and Range.

Table (6): Parameters of variogram function of the spatiotemporal data of Arsenic and Chrome

Parameters \ Data	Metal	Model	Theta or Time	Sill (m^2)	Nugget Effect(m^2)	Range (m or month)
Space	As	Spherical	(0°,90°)	17.58	4.014	6
			(45°,135°)	32.5	7.308	8.485
Spatiotemporal	As	Spherical	t=1	60.01	9.668	6
			t=2	48.87	9.225	8.485
			t=3	66.62	9.829	8.485
Space	Cr	Exponential	(0°,90°)	6.58	0.848	6
			(45°,135°)	7.503	1.154	8.485
Spatiotemporal	Cr	Exponential	t=1	7.775	0.789	6
			t=2	6.58	0.848	8.485
			t=3	6.941	0.803	8.485

Table (6) shows the results of the variogram function parameters for the spatiotemporal data of Arsenic and Chrome. It demonstrates the model approximate to the covariance function through the characteristics of the variogram functions and their means in all the angles with the same lag as mentioned earlier, and it also shows the parameters of all the times (t =1, t =2 and t=3) of the mean of the variogram function of Arsenic and Chrome. The table shows the main parameters of the variogram function with the spatial pattern in the angles (0^o, 90^o) and (45^o,135^o) as the table includes the parameters of variogram parameters as (sill) stands for the variance, (nugget effect) represents the nugget effect, while (range) represents the range with (meter or month). As for the spatiotemporal, it shows (t = 1,2,3) for the data related to the time of the two metals (Arsenic and Chrome).

Table (7): Selected prediction values with the performance of prediction measures

MAPE	0.13244	0.1156	0.1002	0.3372
RMSE	0.1451	0.3219	0.2117	1.0089
Z*(s)	32.574	27.1918	18.2894	25.5074

Table (7) shows some values to be predicted as Z* represents the values to be predicted, and Z stands for the actual values with the standards of error (MAPE and RMSE). From the results, it is noticed that the standards of error are small in value, and this indicates the validity of the prediction process of the data about which prediction rests compared with the original data.

4. Conclusions:

The selection of the mathematical model and the evaluation of the impartiality of the models are necessary to improve the prediction by applying the spatiotemporal data and drawing the curves of the spatiotemporal distribution of arsenic and chromium data in soil pollution in the study area. From **Table (6)**, we notice that the variogram function has the aspherical model in the case of spatial data and spatiotemporal data for arsenic metal, while in the case of spatial and spatiotemporal data, the variogram function has an exponential model in the case of chromium metal. We note that there is a great similarity in the properties of the covariance functions(spherical model and exponential model) through forecasting and taking into account the criteria for the correctness of the prediction as well as the least variance and the conditions of the results obtained in obtaining covariance models with convergent parameters for the best prediction show us the property of uniform spatial distribution of data in all directions of the compass and through the application of the kriging technique, the results showed the correctness of the prediction and the completion methods showed similar performance between the kriging technique. Finally, the proposed model of the spherical curve and the exponential curve

approaches 91% of the model of covariance functions for common spatiotemporal data with very small error rates when forecasting.

Universal kriging (UK), the method of spatial or temporal multiple regression, is a model that divides a random function into a linear set of drift and a random element that is the remainder.

Through this research, we recommend using infection disease data and atmospheric gas pollution data and entering three-dimensional data to obtain a proposed mathematical model and other spatiotemporal forecasting methods and linking them to artificial intelligence methods and the fuzzy method.

5. References

[1] Burrough PA, McDonnell RA, Lloyd CD. Principles of geographical information systems. 3rd ed. London, England: Oxford University Press; 2015.

[2] Camana FA, Deutsch CV. Cokriging of Multiple Types of Drill Hole Data. CCG Annual Report. 2020;22.

[3] Caloiero T, Filice E, Coscarelli R, Pellicone G. A homogeneous dataset for rainfall trend analysis in the Calabria region (Southern Italy). Water. 2020;12.(٩)

[4] Cheng, H., Shen, R., Chen, Y., Wan, Q., Shi, T., Wang, J., ... and Li, X. Estimating

[5] heavy metal concentrations in suburban soils with reflectance

[6] spectroscopy. Geoderma. 2019; 336, 59-67.

[7] Chiles JP, Dilfiner P. Geostatistics: modeling spatial uncertainty. Vol. 713. John Wiley and Sons; 2012.

[8] Collins FC, Bolstad PV. A Comparison of Spatial Interpolation Techniques in Temperature Estimation. In: Proceedings of the 3rd International Conference/Workshop on Integrating GIS and Environmental Modeling. Santa Barbara, Santa Fe, NM; Santa Barbara, CA; 1996.

[9] Cseke B, Zammit-Mangion A, Heskes T, Sanguinetti G. Sparse approximate inference for spatio-temporal point process models. Journal of the American Statistical Association. 2016;111(516):1746–63.

[10] Farmer WH. Ordinary kriging as a tool to estimate historical daily streamflow records. Hydrology and Earth System Sciences. 2016;20(7):2721–35.

[11] Goovaerts P. Kriging and semivariogram deconvolution in the presence of irregular geographical units. Mathematical geosciences. 2008;40:101–28.

[12] Huang CL, Wang HW, Hou JL. Estimating spatial distribution of daily snow depth with kriging methods: combination of MODIS snow cover area data and ground-based observations. The Cryosphere Discussions. 2015;9(5):4997–5020.

[13] Journal AG, Huijbregts CJ. Mining Geostatistic. New York: Academic Press; 1978.

[14] Kilibarda M, Hengl T, Heuvelink GBM, Graler B, Pebesma E, Tadic MP, et al. Spatio-temporal interpolation of daily temperatures for global land areas at 1 km resolution. Journal of Geophysical Research: Atmospheres. 2014;119(5):2294–313.

[15] Kerry, R., Goovaerts, P., Rawlins, B. G., and Marchant, B. P. Disaggregation of legacy soil data using area to point kriging for mapping soil organic carbon at the regional scale. Geoderma. 2012;170, 347-358.

[16] Keskin, H., and Grunwald, S. Regression kriging as a workhorse in the digital soil mapper's toolbox. Geoderma. 2018;326, 22-41.

[17] Kumar V. Kriging of groundwater levels, case study. Journal of Spatial Hydrology. 2006;6:81–94.

[18] Tadić JM, Williams IN, Tadić VM, Biraud SC. Towards hyper- Dimensional variography using the product-sum covariance model. Atmosphere. 2019;10.(٣)

[19] Tan K, Ma W, Wu F, Du Q. Random forest-based estimation of heavy metal concentration in agricultural soils with hyperspectral sensor data. Envirosnmental monitoring and assessment. 2019;191:1–14.

[20] Varadhan R. Numerical optimization in R: Beyond optimization. Journal of Statistical Software. 2014;60:1–3.

[21] Wikle, C. K., Zammit-Mangion, A., and Cressie, N. Spatiotemporal statistics with R. CRC Press.2019 .

[22] Yoon SY, Ravulaparthy SK, Goulias KG. Dynamic diurnal social taxonomy of urban environments using data from a geocoded time use activity-travel diary and point-based business establishment inventory. Transportation Research Part A: Policy and Practice. 2014; 68:3–17.

[23] Zammit-Mangion A. FRK: An R package for spatial and spatiotemporal prediction with large datasets. 2017.